

UC Irvine

UC Irvine Previously Published Works

Title

The functionality and translatability of neocartilage constructs are improved with the combination of fluid-induced shear stress and bioactive factors

Permalink

<https://escholarship.org/uc/item/6rj8p2dm>

Journal

The FASEB Journal, 36(4)

ISSN

0892-6638

Authors

Salinas, Evelia Y
Donahue, Ryan P
Herrera, Jessica M
[et al.](#)

Publication Date

2022-04-01

DOI

10.1096/fj.202101699r

Peer reviewed



Published in final edited form as:

FASEB J. 2022 April ; 36(4): e22225. doi:10.1096/fj.202101699R.

The Functionality and Translatability of Neocartilage Constructs are Improved with the Combination of Fluid-Induced Shear Stress and Bioactive Factors

Evelia Y. Salinas^{+,1}, Ryan P. Donahue^{+,1}, Jessica M. Herrera^{+,2}, Jerry C. Hu¹, Kyriacos A. Athanasiou^{*,1}

¹Department of Biomedical Engineering, 3120 Natural Sciences II, University of California, Irvine, Irvine, CA 92697-2715

²Department of Bioengineering and Therapeutic Sciences, 216 Byers Hall, 1700 Fourth St, University of California, San Francisco, San Francisco, CA 94158

Abstract

Neocartilage tissue engineering aims to address the shortcomings of current clinical treatments for articular cartilage indications. However, advancement is required toward neocartilage functionality (mechanical and biochemical properties) and translatability (construct size, gross morphology, passage number, cell source, and cell type). Using fluid-induced shear (FIS) stress, a potent mechanical stimulus, over four phases, this work investigates FIS stress' efficacy toward creating large neocartilage derived from highly passaged minipig costal chondrocytes, a species relevant to the preclinical regulatory process. In Phase I, FIS stress application timing was investigated in bovine articular chondrocytes and found to improve aggregate modulus of neocartilage by 151% over unstimulated controls when stimulated during the maturation stage. In Phase II, FIS stress stimulation was translated from bovine articular chondrocytes to expanded minipig costal chondrocytes, yielding a 46% improvement in aggregate modulus over nonstimulated controls. In Phase III, bioactive factors were combined with FIS stress to improve the shear modulus by 115% over bioactive factor-only controls. The translatability of neocartilage was improved in Phase IV by utilizing highly passaged cells to form constructs more than 9-times larger in area (11×17mm), yielding an improved aggregate modulus by 134% and a flat morphology compared to free-floating, bioactive factor-only controls. Overall, this study represents a significant step toward generating mechanically robust, large constructs necessary for animal studies, and, eventually, human clinical studies.

*Corresponding author: athens@uci.edu.

⁺Co-first authors.

Contributions

EYS, RPD, and JMH designed the experiments, analyzed the data, drafted the manuscript, and critically edited the manuscript. JCH and KAA oversaw and guided the experiments, drafted the manuscript, and critically edited the manuscript.

Competing Interests

Kyriacos A. Athanasiou and Jerry C. Hu are scientific consultants for Cartilage Inc.

Keywords

articular cartilage; tissue engineering; mechanical stimulation; fluid-induced shear stress; neocartilage

1. Introduction

Articular cartilage is a stiff and resilient tissue that protects bones and distributes forces during movement. Native articular cartilages vary widely in compressive aggregate modulus values, ranging from about 250 kPa to about 1400 kPa depending on the location and species (1–3). Cartilage trauma and wear can cause defects that do not naturally heal (4). Currently, the most common treatments for articular cartilage lesions are chondroplasty and microfracture, neither of which are considered effective for more than 5 years post-treatment (5, 6). If cartilage lesions are not properly treated, they can progress to osteoarthritis (OA). OA currently affects 32 million people in the U.S. and is projected to rise up to 60% in prevalence over the next 20 years (7, 8). Compared to the current short-term solutions applied to cartilage lesions, an emerging solution for articular cartilage defects is tissue engineering, which aims to provide a long-term regenerative solution (4). Additionally, tissue-engineered cartilage derived from expanded cells has the potential to provide an inexhaustible amount of implant material, addressing the major clinical problem of donor tissue scarcity (9). Although several advances in cartilage tissue engineering have been developed over the last several years, including the self-assembling process (9–12), certain improvements must still be made before the successful implantation of neocartilage in humans, such as 1) finding the ideal timing of neocartilage stimulation regimens toward functional improvement, 2) establishing the reproducibility of the effects of mechanical stimuli across multiple species and cell types, 3) exploring the additive effects of multiple types of stimuli (i.e., biochemical and mechanical), and 4) scaling-up of constructs.

Certain magnitudes of mechanical stimulation regimens improve neocartilage tissue properties toward those of native tissue, but the timeline of application is not typically scrutinized. For example, fluid-induced shear (FIS) stress has been previously shown by our group and others to mechano-regulate ion channels on the primary cilia of chondrocytes, leading to enhancements in neocartilage extracellular matrix (ECM) content and mechanical properties (11, 13–16). A previous study investigating the use of FIS stress found that applying 0.05–0.21 Pa of shear stress on neocartilage improved both bovine and human constructs (11); however, the timeline of application is has not been previously investigated. Determining an ideal application window for neocartilage mechanical stimulation is critical because timed mechanical cues help maintain tissue health in native cartilages. For example, during embryonic development, chondrocytes are stimulated by mechanical loading to synthesize ECM (17, 18), and during postnatal development, mechanical loading regulates cartilage thickness and maturation (19, 20). Certain tissue engineering methods, such as the neocartilage self-assembling process, have also been shown to follow similar developmental steps and may exhibit the same maturation-dependent mechanical signaling needs (21–23). For example, self-assembled neocartilage undergoes the synthesis stage (days 7–14), when the chondrocytes produce ECM, and the maturation stage (days 15–22), when production of

glycosaminoglycans is increased and collagen content is decreased (Figure 1a) (23, 24). The maturation-dependency of mechanical stimulation regimens, such as FIS stress, should be investigated toward maximizing mechanical properties of neocartilage (25).

To translate mechanical stimulation technologies to the clinic, the reproducibility of tissue engineering techniques across species and sources must be examined. This is a necessary design criterion because the Food and Drug Administration (FDA) requires analogous products to be tested in animal studies prior to use in human clinical trials. For neocartilages, exploratory experiments may be conducted using bovine articular chondrocytes since they are inexpensive and easily obtainable. Eventually, the species and source will need to be translated to a commonly used preclinical animal model for *in vivo* testing. The Yucatan minipig is considered a suitable animal model for most preclinical work because of its similarity to humans in weight, anatomy, immunology, physiology, and bone biology (26–30). Specifically, it is widely used for cartilage therapeutic testing in articular cartilage, knee meniscus, and temporomandibular joint disc investigations (12, 28, 30, 31). Another consideration is the cell source. For example, costal chondrocytes may be advantageous over articular chondrocytes due to their ability to be harvested autologously and allogeneically without further damaging diseased joints that require treatment. Costal chondrocytes are also advantageous because they regain their chondrogenic phenotype via redifferentiation methods after expansion (32–34). To eventually translate a mechanical stimulus for human use, analogous sources should be tested with an appropriate species that will be used in preclinical studies to satisfy regulatory guidance toward eventual human use.

To improve neocartilage functional properties, exogenous growth factors, enzymes, and other small molecules (i.e., bioactive factors) have been extensively studied to optimize their dosage and timeline of application (35–40). Nevertheless, how bioactive factors work in conjunction with mechanical stimulation is of interest because of the potential for additive improvements in neocartilage functional properties. For example, transforming growth factor beta 1 (TGF- β 1) alone has led to enhanced collagen and glycosaminoglycan synthesis during the self-assembling process (Figure 1b) (37) and in scaffold-based neocartilages (41). TGF- β signaling has been shown to be regulated through the primary cilia (42), the main mode of action of FIS stress (11). This is significant because exogenous TGF- β 1 addition and FIS stress might act in a similar manner to improve ECM content. Other bioactive factors, such as chondroitinase ABC (C-ABC), lysyl oxidase-like 2 (LOXL2), and insulin-like growth factor 1, have been studied in conjunction with TGF- β 1 toward further improving functional properties of neocartilage (43), including self-assembled neocartilage (Figure 1b) (37). Additionally, the use of bioactive factors independently or together with tensile and compressive stimulation has been explored (10, 23, 35), motivating further exploration and combination with other mechanical stimulation regimens, such as FIS stress.

To repair larger cartilage defects, large neocartilage constructs (e.g., 11×17mm) that are mechanically robust and have a flat morphology must be generated, and more cells will be necessary to create these large constructs. While the process of further expanding chondrocytes is simple, recent studies have shown that maintaining a chondrogenic phenotype in highly passaged cells is exceedingly complex due to dedifferentiation (44,

45) and leads to the creation of neocartilage constructs that are not flat (9). For example, protocols for creation of flat, robust neocartilages have been developed using aggregate rejuvenation combined with the use of bioactive factors, such as TGF- β 1, C-ABC, and LOXL2. This work has yielded small constructs that maintain flat morphology and mechanical robustness despite using cells that have been passaged up to 11 times (9). However, further attempts at increasing the size of self-assembled constructs in the past have yielded constructs that fold or become wavy due to the actin cytoskeleton exerting internal tensile forces within the construct (46). In large constructs, the addition of cytochalasin D, a potent inhibitor of actin polymerization, has been shown to yield flat neocartilage construct morphology (Figure 1b) (46). Moreover, cytochalasin D addition has also been known to restore the primary cilia on extensively passaged chondrocytes, which could further enhance the effects of FIS stress in this phase (42). For addressing articular cartilage indications of larger sizes, it will be critical to develop protocols for larger constructs with both biochemical and mechanical stimulation which generate mechanically robust and flat neocartilages.

Toward successful implantation of neocartilage in humans, the global objective of this work was to improve the functional and translational aspects of neocartilage constructs using FIS stress and bioactive factors. In particular, the functional properties investigated were mechanical properties and ECM content, while the translational aspects investigated were construct size (5mm diameter circular vs. 11 \times 17mm rectangular), gross morphology (flat neocartilage), passage number (passages 0, 3, and 6), cell source (bovine vs. minipig), and cell type (articular chondrocytes vs. costal chondrocytes). We hypothesized that the combination of FIS stress and bioactive factors would yield flat, large, neocartilage constructs that are mechanically robust. This series of studies was divided into four phases. In Phase I, the objective was to determine if application of FIS stress during the synthesis stage (days 7–14) or during the maturation stage (days 15–22) of the self-assembling process was most beneficial for biochemical and mechanical properties (Figure 1a). In Phase II, a clinically relevant and widely accepted animal model and cell source (i.e., costal chondrocytes from the Yucatan minipig) were used with the appropriate timing derived from Phase I (28, 30). In Phase III, bioactive factors previously shown to improve functional aspects of neocartilage constructs were used in conjunction with FIS stress with the goal of increased functionality (Figure 1b). Finally, in Phase IV, the combination of FIS stress timing and bioactive factors discovered in Phases I to III was applied to constructs derived from highly passaged minipig costal chondrocytes to create large, flat neocartilage constructs for larger articular cartilage indications.

2. Methods

2.1. Overview of experimental phases

In Phase I, the ideal FIS stress application window was determined by creating neocartilage constructs from bovine articular chondrocytes and stimulating them with FIS stress during the synthesis stage (days 7–14), maturation stage (days 15–22), or a combination of both stages (days 11–18) (Figure 1a). In Phase I, nonstimulated neocartilage created from bovine articular chondrocytes served as a control group. Next, in Phase II, Yucatan minipig costal

chondrocytes were expanded to passage 3 and used to create neocartilage constructs that were either stimulated with FIS stress during the optimal period or not stimulated with FIS stress. In Phase III, the combination of FIS stress and bioactive factors (TGF- β 1, C-ABC, and LOXL2) was investigated to further improve functionality of neocartilage constructs created from Yucatan minipig costal chondrocytes. Bioactive factors were included in the creation of all the neocartilage constructs for Phase III, including controls. Finally, in Phase IV, the results from all previous phases were used to create large (11 \times 17mm), neocartilage constructs from highly passaged Yucatan minipig costal chondrocytes.

2.2. Isolation of bovine articular chondrocytes

For Phase I of this study, bovine articular chondrocytes were isolated by mincing cartilage from the femoral condyles and trochlear grooves of the knees of six, 2-month old Jersey calves. Mincing pieces from each leg were stored in 30ml of wash medium, which consisted of Dulbecco's Modified Eagle's Medium (DMEM) and 1% penicillin-streptomycin-fungizone (PSF). The minced tissue from each leg was washed 2–3 times with wash medium and digested in a petri dish using collagenase II solution (0.2% w/v, Worthington Biochemical's Collagenase type II in wash medium, 3% fetal bovine serum (FBS)) for 18hr on an orbital shaker at 37°C at 60RPM. Following this, the solution with cells was filtered through 70 μ m cell strainers and centrifuged for 5 minutes at 400g to remove the collagenase. The resulting cell pellet was washed with phosphate-buffered saline (PBS). The chondrocytes were then washed with ammonium-chloride-potassium (ACK) lysis buffer, followed by several washes with PBS (47). Finally, chondrocytes were counted and frozen in 90% FBS and 10% dimethyl sulfoxide (DMSO) for downstream self-assembly.

2.3. Isolation of minipig costal chondrocytes

For Phases II, III, and IV of this study, minipig costal cartilage was obtained from three, 6-month old Yucatan minipigs. Costal cartilage was minced into \sim 1mm³ pieces. The cartilage pieces were then digested with pronase solution (0.4% w/v, in wash medium, 3% FBS) for 1hr followed by 18hr in collagenase II solution on an orbital shaker at 60RPM. Finally, the cells were strained, treated with ACK lysis buffer, washed several times, counted, and frozen in 90% FBS and 10% DMSO either immediately as primary cells or after one passage, as previously described (12).

2.4. Passaging and aggregate rejuvenation of minipig costal chondrocytes

Cell vials were thawed by placing in a 37°C water bath and adding cells drop-wise to wash medium to ensure high viability. The tubes were spun down at 400g for 5 minutes, and cells were resuspended in pre-warmed chondrogenic medium (CHG), which consisted of DMEM, 1% PSF, 1% nonessential amino acids, 1% insulin-transferrin-selenous acid, 50 μ g/ml ascorbate-2-phosphate, 40 μ g/ml L-proline, 100 μ g/ml sodium pyruvate, and 100nM of dexamethasone. The cells were seeded in 27ml per flask of CHG, plus 2% FBS and growth factors (1ng/ml TGF- β 1 + 5ng/ml basic fibroblast growth factor + 10ng/ml platelet derived growth factor), at 2.5 million cells per flask. Finally, the flasks were checked for confluence every 1–2 days, and the cells were fed every 3–4 days with CHG, plus 2% FBS and growth factors.

The cells were passaged every two weeks or until the cells were confluent, whichever came first. Cells for Phase II and III were expanded to passage 3, while Phase IV utilized passage 6 cells. Wash medium was added to each flask to rinse, and, subsequently, 0.05% Trypsin-EDTA was added to each flask. The flasks were placed in an incubator for 8–9 minutes, and wash medium, plus 10% FBS, was added to the growth surface of the flask to neutralize the Trypsin-EDTA. The suspension of cells were spun down, and the supernatant was discarded. The cell pellet was resuspended in collagenase II solution and placed in a 37°C water bath. The cell suspension was pipetted up and down every 10–15 minutes for 20–30 minutes. The cell suspension was spun down to remove the supernatant, and the cells were counted in wash medium. The cells were plated for the next passage until the terminal passage when they were placed into aggregate rejuvenation. The three individual costal chondrocyte donors were passaged individually until the last passage when they were combined for the remainder of culture.

Finally, the cells were then placed into aggregate rejuvenation, which allowed the cells to recover their chondrogenic phenotype (48). Petri dishes were coated with molten 1% agarose to create a nonadherent surface. The cells were seeded at a final density of 750 thousand cells per ml of medium in 30ml (22.5 million cells per dish) of CHG plus growth factors (10 ng/ml TGF- β 1 + 100ng/ml growth differentiation factor 5 + 100ng/ml bone morphogenetic protein 2). The petri dishes were placed on an orbital shaker for 24hrs at 50RPM, then subsequently cultured under static conditions. The aggregates were fed every 3–4 days for 14 or 11 days for Phases II/III or IV, respectively. It has been previously shown that expanded chondrocytes that are placed in aggregate rejuvenation maintain a chondrogenic phenotype throughout the self-assembling process, exhibiting high expression of aggrecan, collagen type II, and SRY-box transcription factor 9 and minimal expression of osteocalcin and collagen type I (49).

2.5. Self-assembly of neocartilage constructs

Custom made well-makers were used to make negative molds in 2% agarose wells. CHG was added and exchanged twice before seeding chondrocytes. Wells were 5mm diameter cylinders for Phases I, II, and III. For Phase IV, wells were scaled-up from prior studies to 11×17mm rectangular wells (10, 24). As described previously, chondrocytes were seeded into the 2% agarose wells at densities of 4 million bovine chondrocytes per well for Phase I, 2 million minipig chondrocytes per well for Phases II and III, and 15 million minipig chondrocytes per well for Phase IV to begin the self-assembling process. After seeding, 0.5ml of CHG was added to each well in Phases I, II, and III, while 5ml of CHG was added to each well for Phase IV, at the 4hr timepoint. Seven or two days after seeding for small circular or large rectangular constructs, respectively, the self-assembled neocartilage constructs were unconfined from the agarose wells and cultured in 24- or 6-well plates. The small circular and large rectangular constructs received changes of medium (0.5ml or 5.0ml) every day up until unconfining, and 1ml or 10ml of medium on alternating days for the remainder of the 28 day culture period.

2.6. FIS stress stimulation and devices

FIS stress was applied to the treatment groups by placing the neocartilage constructs in a FIS stress device at the previously specified stages of maturation (Table 1). The device for 5mm neocartilage constructs was created by adding 25ml of 3% agarose to a 100×25mm petri dish, placing the device mold to create small protruding agarose poles, and removing the mold once the agarose solidified, as described previously (11). Each of the neocartilage constructs were positioned between four surrounding poles to keep the constructs in place, and 20ml of CHG was added to the device (Figure 2a). A new device was created for the stimulation of 11×17mm neocartilage constructs using an acrylic base and stainless-steel metal rods (Figure 2b). As with the original device, the new device was designed to be placed inside a petri dish (100×25mm), and the neocartilage constructs were loaded into the device. Acrylic weights were also used to hold the neocartilage constructs in place (Figure 2b). Three constructs were loaded per FIS stress device, and 30ml of CHG was added to the device. The FIS stress device was then placed on an orbital shaker at 50RPM, and, as the orbital shaker rotated, it allowed the medium in the FIS stress device to flow over the neocartilage constructs, thereby applying 0.05–0.21Pa of FIS stress, as previously characterized (11). Since both devices were designed to have the same radius and are placed on the orbital shaker at the same rotational speed, the fluid-flow and resulting FIS stress applied to the neocartilage constructs are not altered, as is shown by previous computational fluid dynamic modeling studies (50–53).

2.7. Bioactive factor treatment

The timeline of application for bioactive factor treatment is summarized in Table 1. The use of these bioactive factors was used in accordance with previous studies showing that 1) bioactive factors improved the functional properties of self-assembled constructs (9, 10, 12, 24, 35, 37, 46, 54, 55) and 2) bioactive factors improved flatness of large constructs derived from highly passaged cells (35, 46). For Phase III, TGF- β 1 (10ng/ml) was applied for the entire duration of the 28 days of self-assembly, while C-ABC (2.0U/ml) was applied on day 7 for 4hr to temporarily deplete glycosaminoglycan content, as previously described (55). LOXL2 was applied at 0.15 μ g/ml in conjunction with copper sulfate (1.6 μ g/ml) and hydroxylysine (0.146mg/ml) from days 7–21. For Phase IV, the culture time was extended to 42 days to maximize construct thickness and mechanical properties; LOXL2 treatment was extended until the end of culture and C-ABC was treated as described above. TGF- β 1 was modified for large constructs in Phase IV to be applied after unconfining (day 2) for the remaining duration of the culture, and cytochalasin D (2 μ M) was applied from days 1–3, as previously described (46).

2.8. Analysis of mechanical properties

After completion of culture, mechanical testing of the neocartilage constructs was performed. To determine the compressive properties, a circular 2mm diameter punch was taken from the center of the construct, and a creep indentation test was performed to determine aggregate modulus and shear modulus, as previously described (56). For Phase IV, 3mm diameter circular punch specimens were also examined in a compressive stress-relaxation test at 10% strain on a uniaxial Instron machine (Model 5665) to determine the

instantaneous modulus and relaxation modulus, as determined from a standard linear solid model using MATLAB software (30).

Tensile testing was conducted using an uniaxial Instron machine, as previously described (57). Neocartilage constructs were cut into dog bone-shaped samples and were glued to paper tabs with a predefined gauge length of 1.55mm. The thickness and width of the dog bone-shaped samples were measured using ImageJ, and a subsequent cross-sectional area was calculated. A uniaxial strain-until-failure test was conducted with a strain rate of 1% per second. Load–displacement curves were normalized to the cross-sectional area and gauge length of each sample. Finally, the Young’s modulus and ultimate tensile strength were calculated using MATLAB software.

2.9. Analysis of biochemical properties

For ECM content, wet weight (WW) and dry weight (DW) of the samples were measured, and specific assays were used to quantify collagen content and glycosaminoglycan content. First, the samples were frozen to allow for sublimation during a 72hr lyophilization cycle. After lyophilization, DWs were measured, and the tissue was digested in a buffered papain solution for 18hr at 65°C. The glycosaminoglycan and collagen contents were normalized per WW and is reported in percentage. Glycosaminoglycan content was measured using a BioColor Blyscan glycosaminoglycan assay kit according to the manufacturer’s directions. The total collagen content was measured using a modified chloramine T hydroxyproline assay and a Sircol collagen standard, as previously described (58).

2.10. Histology

Construct samples from Phase IV were fixed in 10% neutral buffered formalin for at least 48hr immediately after culture completion. Samples were then processed, embedded in paraffin, and sectioned at 5µm for subsequent staining with hematoxylin and eosin (H&E), safranin O (Saf O) with fast green counterstain, and picrosirius red (Picro Red).

2.11. Statistics

For Phase I, one-way analysis of variance (ANOVA) and Tukey’s *post hoc* tests were performed using $p < 0.05$ to determine statistically significant differences among groups. Groups deemed significantly different by the Tukey’s *post hoc* tests are denoted using alphabetical letters via a connecting letters report, where groups not sharing the same letter are statistically significant. For Phases II, III, and IV, Student’s *t*-test was used at $p < 0.05$ to determine statistically significant differences between groups.

3. Results

3.1. Phase I: FIS stress stimulation during the maturation stage yields the largest functional increases over nonstimulated controls

To determine which stimulation time would lead to the most mechanically robust neocartilage constructs, FIS stress was applied at the different stages of neocartilage development (Figure 1a). For the compressive stiffness, the neocartilage constructs stimulated during the maturation stage improved 2.51-times over the nonstimulated

control in aggregate modulus values ($p < 0.0001$) (Figure 3a). They also trended higher than the neocartilage constructs stimulated during the combination stage (Figure 3a). When considering tensile properties, neocartilage stimulated during the maturation and combination stages saw improvements in ultimate tensile strength over nonstimulated controls, showing an 100% increase ($p = 0.0185$ and $p = 0.0144$, respectively) (Figure 3b). In parallel, collagen content of constructs stimulated during the maturation stage was improved over the collagen content of nonstimulated neocartilage ($p < 0.0001$), exhibiting an 82% increase (Figure 3c). Toward achieving the maximal improvement in neocartilage biochemical and mechanical properties, FIS stress stimulation during the maturation stage was selected to move forward to Phases II through IV.

3.2. Phase II: FIS stress yields similar neocartilage functional increases using expanded and rejuvenated minipig costal chondrocytes

To evaluate the translatability of FIS stress stimulation across chondrocytes from different sources and species, Phase II explored the use of Yucatan minipig costal chondrocytes to produce neocartilage constructs. As in Phase I, neocartilage derived from Yucatan minipig costal chondrocytes was stimulated during the maturation stage. Compressive properties were examined, and it was found that the aggregate modulus values of neocartilage stimulated with FIS stress during the maturation stage were 46% higher than nonstimulated neocartilage ($p = 0.0020$) (Figure 4a). Furthermore, tensile properties were also improved; the ultimate tensile strength of neocartilage stimulated with FIS stress during the maturation stage was 78% higher than that of nonstimulated neocartilage ($p = 0.0002$) (Figure 4b). Similarly, the Young's modulus of neocartilage stimulated with FIS stress during the maturation stage was 78% higher than nonstimulated neocartilage ($p = 0.0041$) (Figure 4b). An improvement in Young's modulus had not been previously seen in self-assembled neocartilage constructs made with bovine articular chondrocytes stimulated with FIS stress. As in neocartilage created with bovine neocartilage constructs in Phase I, an increase in glycosaminoglycan content was observed in minipig neocartilage stimulated during the maturation stage compared to the nonstimulated control (Figure 4c); a 136% increase in glycosaminoglycan content was observed ($p = 0.0008$). Interestingly, although collagen content trended higher, a significant increase in collagen content was not observed in the FIS stress-stimulated neocartilage created with minipig costal chondrocytes (Figure 4c). As the Yucatan minipig is a widely used preclinical model for treatment of cartilage lesions (12, 28, 30, 31), this phase showed that FIS stress can be applied across various sources and species for similar functional improvements.

3.3. Phase III: Bioactive factors in conjunction with FIS stress yield further functional improvements over bioactive factors alone

Bioactive factors have been previously found to further enhance neocartilage constructs (37), and they were applied here in conjunction with FIS stress toward further functional improvement. FIS stress in combination with bioactive factor treatment significantly increased aggregate modulus ($p = 0.0006$) and shear modulus ($p < 0.0001$) values by 48% and 115%, respectively, over bioactive factor-only controls (Figure 5a). Both measures of tensile properties, Young's modulus and ultimate tensile strength, were also significantly higher with application of FIS stress and bioactive factors compared to bioactive factor-only

controls ($p=0.0047$ and $p=0.0014$, respectively) (Figure 5b). In terms of ECM content, glycosaminoglycan and collagen content were measured (Figure 5c); glycosaminoglycan content was significantly higher ($p<0.0001$) with the application of FIS stress and bioactive factors compared to bioactive factor-only controls. The combination of bioactive factors and FIS stress led to improved neocartilage properties when compared to bioactive factors alone. However, when comparing the magnitudes of aggregate modulus and Young's modulus values of the FIS stress plus bioactive factor group of Phase III to those from the FIS stress-stimulated group of Phase II, the neocartilage properties did not further improve when stimulated with bioactive factors. However, application of bioactive factors is important for examining large constructs as it has been previously demonstrated that rejuvenated constructs stimulated with bioactive factors yield mechanically robust and flat constructs (9), an important clinical feature for tissue-engineered cartilage therapeutics. Despite this, stimulation with bioactive factors and FIS stress yielded improved functionality when compared to neocartilage stimulated with only bioactive factors.

3.4. Phase IV: Large constructs derived from highly passaged cells are mechanically robust and flat

Phase IV examined the effect of FIS stress in conjunction with bioactive factors on large rectangular 11×17 mm neocartilage constructs derived from passage 6 costal chondrocytes. Although the functional properties of neocartilage stimulated with a combination of FIS stress and bioactive factors in Phase III did not significantly improve over FIS stress-stimulated groups of Phase II, the addition of bioactive factors and cytochalasin D has previously been necessary to create neocartilage constructs larger than 5mm diameter, specifically when using highly passaged chondrocytes (9, 46). Compressive properties were examined using both creep indentation and stress-relaxation. Aggregate modulus increased 2.34-times over bioactive factor-only controls ($p=0.0251$), while shear modulus increased 2.72-times over controls ($p=0.0064$) (Figure 6a). Under 10% strain, the relaxation modulus significantly increased by 100% ($p=0.0251$) and the instantaneous modulus did not significantly differ (Figure 6a). The constructs were also measured under uniaxial tension in both axes (i.e., short and long) (Figure 2b). The only significant difference was in the short axis Young's modulus, which increased significantly when stimulated with FIS stress over bioactive factor-only controls ($p=0.0216$). For biochemical content, collagen increased when treated with FIS stress compared to bioactive factor-only controls ($p=0.0209$) (Figure 6c). While glycosaminoglycan trended upwards with application of FIS stress, it was not significant (Figure 6c). Compared to free-floating constructs stimulated only with bioactive factors, those to which FIS stress was applied exhibited a flatter morphology and less curling (Figure 6d). Histologically, samples stimulated with FIS stress and bioactive factors had increased staining intensity in Saf O (Figure 7a), indicative of neocartilage constructs with more glycosaminoglycan content, but similar staining intensities under H&E (Figure 7b). Picro Red staining shows spatial organization of collagens within the matrix. The groups seem to have similar overall intensities, but FIS stress increased the peripheral staining, indicating stronger collagen deposition on the outer edges of the neocartilage constructs (Figure 7c). These staining trends from Figure 7 follow those quantitative metrics for glycosaminoglycan and total collagen content presented in Figure 6c. Combined, these results indicate that large constructs derived from highly passaged cells respond in a

similar manner to the combination of bioactive factors and FIS stress during the maturation stage compared to small constructs from Phases I through III. Additionally, mechanical confinement in the form of the novel FIS stress device also improves construct flatness. This represents a significant step toward treating larger articular cartilage defects using large constructs.

4. Discussion

In this series of studies, the global objective of this work was to improve the functional and translational aspects of neocartilage constructs. Specifically, this work tackled four critical aspects of neocartilage engineering across the four phases presented, including 1) finding the ideal application window of FIS stress stimulation for biochemical and mechanical improvement, 2) establishing the reproducibility of FIS stress stimulus across bovine and minipig cell sources, 3) exploring the beneficial effects of combining FIS stress and bioactive factors, and 4) scaling-up the size of neocartilage constructs using highly passaged cells while maintaining a flat morphology and other improvements in functional properties seen with application of FIS stress and bioactive factors. Overall, it was hypothesized that the appropriate combination of FIS stress and bioactive factors would yield flat, large neocartilage constructs with improved mechanical properties and ECM content. Indeed, both the functional characteristics (mechanical properties and ECM content) and the translational aspects (construct size, gross morphology, passage number, cell source, and cell type) were improved. Namely, in Phase I, FIS stress applied during the maturation stage improved compressive stiffness by 151%, tensile stiffness by 45%, and collagen content by 82% in self-assembled neocartilage constructs engineered from bovine articular cartilage cells. In Phase II, the FIS stress stimulation regimen from Phase I was implemented using costal chondrocytes from the Yucatan minipig and also led to similar increases in compressive stiffness (46%) and tensile stiffness (78%). Then, in Phase III, the combination of FIS stress with bioactive factors improved the compressive stiffness (48%) and tensile stiffness (94%) of neocartilage constructs over bioactive factor-only controls. Finally, in Phase IV, the methods from Phases I through III were combined to engineer large neocartilage constructs derived from highly passaged cells, while maintaining the earlier increases seen via application of FIS stress and bioactive factors.

Toward achieving native tissue functionality, the ideal window of FIS stress time of application was identified. This objective is significant because, in native articular cartilage, chondrocytes depend on mechanical loading during embryonic development to synthesize ECM (17, 18), and, during postnatal development, timed mechanical signaling regulates cartilage thickness and maturation for proper function (19, 20). Similarly, previous studies showed that self-assembled neocartilage also follows chronological steps and may exhibit maturation-dependent mechanical signaling needs (22, 23). For example, when nonstimulated neocartilage constructs enter the maturation stage, the production of glycosaminoglycan is increased, whereas collagen content shows a stark decrease (23). In contrast, when FIS stress is applied during the maturation stage (days 15–22) in Phase I of this work, collagen content increased by 82% over nonstimulated constructs and by 33% over constructs stimulated during the synthesis stage (days 7–14). The neocartilage constructs also improved in compressive and tensile properties. These results indicate that,

like native cartilage, carefully timed mechanical signaling is crucial to the development of robust neocartilage. Although further study is necessary to determine the precise pathways leading to these results, FIS stress has been previously shown to activate ECM producing protein pathways via the perturbation of the PC1/PC2 complex on the primary cilia of chondrocytes (11, 15, 16, 59). Inasmuch as previous studies on self-assembled cartilage have seldom investigated time of application of mechanical stimulation, this study showed that stimulation during the maturation stage is optimal in terms of producing a mechanically robust neocartilage suitable for preclinical *in vivo* implantation toward eventual FDA approval for human studies.

As specified by the FDA, tissue-engineered therapeutics must undergo preclinical studies in an appropriate animal model prior to human clinical studies, and, for these, an analogous animal product should be investigated. Therefore, an important translational feature of this study is the demonstration that the FIS stress stimulus is efficacious in an animal model, such as the Yucatan minipig. Furthermore, transferring the FIS stress stimulus to a different cell type, namely, costal chondrocytes, is significant for translation because of their ability to be harvested autologously and allogeneically without further damaging diseased joints that require treatment. For example, in a recent study using bioactive factor-stimulated constructs derived from costal cartilage, the Yucatan minipig was used as a model for temporomandibular joint disc cartilage repair (12). Similarly, several researchers are performing *in vivo* meniscus and articular cartilage repair in the minipig (60–62). Here, constructs were generated from the costal cartilage of the Yucatan minipig and stimulated during the maturation stage. Similar to constructs derived from bovine articular chondrocytes, compressive stiffness and tensile strength and stiffness of minipig-derived neocartilage significantly increased by 46%, 78%, and 78%, respectively, when FIS stress was applied. Although increases in shear modulus are similar between Phases I and II, aggregate modulus increases were larger in Phase I compared to Phase II. These differences are most likely due to changes in the ECM-producing capacity of the different cell types (i.e., articular vs. costal chondrocytes) when stimulated with FIS stress. For example, the increases in collagen are also different between the two phases. Despite these small differences, these are significant results because, 1) FIS stress has not been previously investigated in the costal cartilage cell source, and 2) the Yucatan minipig is a widely used preclinical model. Previous studies have also corroborated the findings shown here that FIS stress stimulation, as well as tensile stimulation, of self-assembled constructs can be translated across cell passage numbers and species (e.g., bovine and human articular chondrocytes) (10, 11). Although additional studies examining FIS stress during the maturation stage in human costal chondrocytes will eventually need to be performed, the work done here shows promise that use of FIS stress on neocartilage would be feasible and beneficial across different cell passage numbers, cell sources, and cell types.

Previously identified cocktails of bioactive factors have been shown to individually improve functionality and morphology of neocartilage constructs (9, 37), but their interactions with FIS stress have not been previously investigated. This is of scientific interest because healthy cartilage, whether native or engineered, is dependent on a variety of signals which include both mechanical and biochemical cues (19, 20, 22, 23, 35–40). Phases III and IV relied on a plethora of past studies which used bioactive factors, employing the regimens

described here, to improve the functional properties of self-assembled cartilage compared to nonstimulated controls (35–39, 46, 63). Here, the addition of bioactive factors (TGF- β 1, C-ABC, and LOXL2) was investigated in combination with FIS stress stimulation to further improve the functional properties of neocartilage constructs and, eventually, keep constructs derived from high passage cells flat. Indeed, it was found that, similar to Phase II, increases were observed in Phase III when FIS stress was combined with bioactive factors, increasing compressive stiffness (by 48%) and tensile stiffness (by 94%). It appears that FIS stress dominates the functional increases seen in constructs regardless of bioactive factor stimulation. As previously shown (9, 10, 12, 24, 35, 37, 46, 54, 55), future studies should include a direct comparison between bioactive factor-stimulated and nonstimulated groups to ensure that the beneficial effects of bioactive factors are maintained in the Yucatan minipig costal cartilage source. The increases in mechanical properties seen here may be due to increased perfusion of growth factors in neocartilage by FIS stress, but this is unknown as the perfusion rates in FIS stress-stimulated neocartilage constructs have not been explored (11). However, previous studies have shown that the primary cilia is implicated in both TGF- β signaling and FIS stress stimulation. Future studies should determine whether perfusion, primary cilia perturbation, or a combination is the exact cause of further improved functional properties of neocartilage constructs (42). The findings of this study mirror the results of previous studies which used these bioactive factors in conjunction with other mechanical stimuli, such as tension and compression (10, 24). For example, combination of passive axial compression and bioactive factors yielded significantly higher relaxation modulus values compared to bioactive factor-only controls (24). Additionally, previous studies have shown that bioactive factors are an important element for maintaining mechanical robustness for highly passaged cells and large constructs (9, 46). Thus, the combination of FIS stress and bioactive factors is important when considering generation of self-assembled neocartilages larger than 5mm in diameter.

Toward addressing larger cartilage lesions, this study examined creation of large, flat, mechanically robust constructs generated from highly passaged costal chondrocytes stimulated with bioactive factors and FIS stress. This phase represents a significant step toward functional and translational improvements for implantation by increasing the tissue-engineered implant in size from 5mm diameter to 11 \times 17mm, representing more than a 9-times increase in construct area. This increase in size also increased the number of cells needed by 7.5-times. Therefore, in Phase IV, in order to accommodate for the high number of cells needed (i.e., 15 million per construct), the number of passages costal chondrocytes undergo, compared to Phases II and III, was doubled from three to six. Although this may seem straightforward, as passage number increases, it has been shown that the cells undergo more dedifferentiation toward a fibroblastic phenotype (64). Using the expansion and aggregate rejuvenation process described (i.e., no bioactive factors), constructs up to passage 5 have exhibited flat morphologies, but then started to display unwanted morphological characteristics at passage 7 (e.g., decreased diameter, biconcave structure) (9). This same study further examined bioactive factor use, as described here, during self-assembly of small 5mm diameter constructs and noted additional increases in functional properties, especially for higher passage constructs, and maintenance of a flat morphology (9). While 5mm diameter constructs remained relatively flat, larger constructs of 25mm diameter did

not remain flat due to internal stresses through the actin cytoskeleton, applying forces to the ECM (46). Previous studies noted that application of bioactive factors, cytochalasin D (an actin polymerization inhibitor), and mechanical confinement in the form of an agarose coverslip are necessary to maintain flatness (46). Cytochalasin D was applied here in a similar regimen toward keeping constructs flat, but it has also been shown to recover primary cilia of chondrocytes after passaging (65), thus, potentially making cytochalasin D-treated cells here more sensitive to FIS stress to yield further increases in functional properties. Similarly, this study showed that mechanical confinement in the form of the novel FIS stress device was necessary to keep constructs flat. As expected, the FIS stress system and other bioactive factors also maintained the functional properties seen in earlier phases of this study. Thus, the combination of highly passaged cells with FIS stress and bioactive factors was successful in generating mechanically robust neocartilage constructs toward improving the range of cartilage lesion indications that can be potentially addressed by self-assembled neocartilage.

This work represents substantial progress toward generating a tissue-engineered neocartilage solution for addressing articular cartilage lesions. Using FIS stress, functional properties, such as aggregate modulus and collagen content, of constructs derived from primary bovine articular chondrocytes and passaged and rejuvenated minipig costal chondrocytes were improved toward native tissue values. For example, compressive aggregate modulus values reported here for neocartilages range from approximately 120–600 kPa. These values are within the range reported for native articular cartilages (250–1400 kPa) (1–3). Additionally, bioactive factors have been previously used in conjunction with other forms of mechanical stimuli (i.e., passive axial compression and tension), but have not been examined in combination with FIS stress, as performed here. The addition of bioactive factors with FIS stress stimulation did not adversely affect functional improvements when compared to bioactive factor-only controls. Finally, combining all the previous phases, large constructs derived from highly passaged costal chondrocytes exhibited mechanical robustness and flatness, important translational features. Combined, the four phases of this study represent significant steps toward generating mechanically robust, flat, large neocartilage constructs necessary for a wide range of preclinical animal studies, and, eventually, human clinical studies for various articular cartilage indications.

Funding Sources

This work was funded by the National Institutes of Health (R01 DE015038, R01 AR078389, R01 AR067821). Evelia Y. Salinas was also in part supported by a National Institutes of Health Diversity Supplement (on R01 AR067821). Jessica M. Herrera was also in part supported by the California Alliance for Minority Participation.

Data Availability Statement

The data that support the findings of this study are available in the article.

References

1. Athanasiou KA, Agarwal A, Muffoletto A, Dzida FJ, Constantinides G, and Clem M (1995) Biomechanical Properties of Hip Cartilage in Experimental Animal Models. *Clinical Orthopaedics and Related Research*, 254–266

2. Athanasiou KA, Liu GT, Lavery LA, Lanctot DR, and Schenck RC Jr. (1998) Biomechanical topography of human articular cartilage in the first metatarsophalangeal joint. *Clin Orthop Relat Res*, 269–281 [PubMed: 9553561]
3. Zimmerman BK, Bonnevie ED, Park M, Zhou Y, Wang L, Burris DL, and Lu XL (2015) Role of interstitial fluid pressurization in TMJ lubrication. *J Dent Res* 94, 85–92 [PubMed: 25297115]
4. Huey DJ, Hu JC, and Athanasiou KA (2012) Unlike bone, cartilage regeneration remains elusive. *Science* 338, 917–921 [PubMed: 23161992]
5. Huang BJ, Huey DJ, Hu JC, and Athanasiou KA (2017) Engineering biomechanically functional neocartilage derived from expanded articular chondrocytes through the manipulation of cell-seeding density and dexamethasone concentration. *J Tissue Eng Regen Med* 11, 2323–2332 [PubMed: 27138113]
6. McCormick F, Harris JD, Abrams GD, Frank R, Gupta A, Hussey K, Wilson H, Bach B Jr., and Cole B (2014) Trends in the surgical treatment of articular cartilage lesions in the United States: an analysis of a large private-payer database over a period of 8 years. *Arthroscopy* 30, 222–226 [PubMed: 24485115]
7. Centers for Disease Control and Prevention. (2020) Osteoarthritis. Vol. 2020, CDC, CDC
8. Centers for Disease Control and Prevention. (2018) Arthritis-Related Statistics. CDC, CDC
9. Kwon H, Brown WE, O’Leary SA, Hu JC, and Athanasiou KA (2021) Rejuvenation of extensively passaged human chondrocytes to engineer functional articular cartilage. *Biofabrication*
10. Lee JK, Huwe LW, Paschos N, Aryaei A, Gegg CA, Hu JC, and Athanasiou KA (2017) Tension stimulation drives tissue formation in scaffold-free systems. *Nat Mater* 16, 864–873 [PubMed: 28604717]
11. Salinas EY, Aryaei A, Paschos N, Berson E, Kwon H, Hu JC, and Athanasiou KA (2020) Shear stress induced by fluid flow produces improvements in tissue-engineered cartilage. *Biofabrication* 12, 045010 [PubMed: 32640430]
12. Vapniarsky N, Huwe LW, Arzi B, Houghton MK, Wong ME, Wilson JW, Hatcher DC, Hu JC, and Athanasiou KA (2018) Tissue engineering toward temporomandibular joint disc regeneration. *Sci Transl Med* 10, 1–10
13. Gemmiti CV, and Guldberg RE (2009) Shear stress magnitude and duration modulates matrix composition and tensile mechanical properties in engineered cartilaginous tissue. *Biotechnology and Bioengineering* 104, 809–820 [PubMed: 19591192]
14. Gemmiti CV, and Guldberg RE (2006) Fluid flow increases type II collagen deposition and tensile mechanical properties in bioreactor-grown tissue-engineered cartilage. *Tissue Engineering* 12, 469–479 [PubMed: 16579680]
15. Ruhlen R, and Marberry K (2014) The chondrocyte primary cilium. *Osteoarthritis and Cartilage* 22, 1071–1076 [PubMed: 24879961]
16. Wann AK, Zuo N, Haycraft CJ, Jensen CG, Poole CA, McGlashan SR, and Knight MM (2012) Primary cilia mediate mechanotransduction through control of ATP-induced Ca²⁺ signaling in compressed chondrocytes. *The FASEB Journal* 26, 1663–1671 [PubMed: 22223751]
17. Bastow ER, Lamb KJ, Lewthwaite JC, Osborne AC, Kavanagh E, Wheeler-Jones CP, and Pitsillides AA (2005) Selective activation of the MEK-ERK pathway is regulated by mechanical stimuli in forming joints and promotes pericellular matrix formation. *J Biol Chem* 280, 11749–11758 [PubMed: 15647286]
18. Dowthwaite G, Flannery C, Flannelly J, Lewthwaite J, Archer C, and Pitsillides A (2003) A mechanism underlying the movement requirement for synovial joint cavitation. *Matrix Biology* 22, 311–322 [PubMed: 12935816]
19. Brama PAJ, TeKoppele JM, Beekman B, van El B, Barneveld A, and van Weeren PR (2000) Influence of development and joint pathology on stromelysin enzyme activity in equine synovial fluid. *Annals of the Rheumatic Diseases* 59, 155 [PubMed: 10666176]
20. Athanasiou KA, Darling EM, DuRaine GD, Hu JC, and Reddi AH (2017) *Articular Cartilage*, CRC Press
21. Kim IG, Ko J, Lee HR, Do SH, and Park K (2016) Mesenchymal cells condensation-inducible mesh scaffolds for cartilage tissue engineering. *Biomaterials* 85, 18–29 [PubMed: 26854388]

22. Athanasiou KA, Eswaramoorthy R, Hadidi P, and Hu JC (2013) Self-organization and the self-assembling process in tissue engineering. *Annu Rev Biomed Eng* 15, 115–136 [PubMed: 23701238]
23. Ofek G, Revell CM, Hu JC, Allison DD, Grande-Allen KJ, and Athanasiou KA (2008) Matrix development in self-assembly of articular cartilage. *PLoS One* 3, e2795 [PubMed: 18665220]
24. Huwe LW, Sullan GK, Hu JC, and Athanasiou KA (2018) Using Costal Chondrocytes to Engineer Articular Cartilage with Applications of Passive Axial Compression and Bioactive Stimuli. *Tissue Eng Part A* 24, 516–526 [PubMed: 28683690]
25. Salinas EY, Hu JC, and Athanasiou K (2018) A Guide for Using Mechanical Stimulation to Enhance Tissue-Engineered Articular Cartilage Properties. *Tissue Eng Part B Rev* 24, 345–358 [PubMed: 29562835]
26. Panepinto LM, and Phillips RW (1986) The Yucatan miniature pig: characterization and utilization in biomedical research. *Lab Anim Sci* 36, 344–347 [PubMed: 3534436]
27. Gutierrez K, Dicks N, Glanzner WG, Agellon LB, and Bordignon V (2015) Efficacy of the porcine species in biomedical research. *Front Genet* 6, 293–293 [PubMed: 26442109]
28. Pfeifer CG, Fisher MB, Saxena V, Kim M, Henning EA, Steinberg DA, Dodge GR, and Mauck RL (2017) Age-Dependent Subchondral Bone Remodeling and Cartilage Repair in a Minipig Defect Model. *Tissue Eng Part C Methods* 23, 745–753 [PubMed: 28747146]
29. Gotterbarm T, Breusch SJ, Schneider U, and Jung M (2008) The minipig model for experimental chondral and osteochondral defect repair in tissue engineering: Retrospective analysis of 180 defects. *Laboratory Animals* 42, 71–82 [PubMed: 18348768]
30. Vapniarsky N, Aryaei A, Arzi B, Hatcher DC, Hu JC, and Athanasiou KA (2017) The Yucatan Minipig Temporomandibular Joint Disc Structure-Function Relationships Support Its Suitability for Human Comparative Studies. *Tissue Eng Part C Methods* 23, 700–709 [PubMed: 28548559]
31. Fisher MB, Belkin NS, Milby AH, Henning EA, Bostrom M, Kim M, Pfeifer C, Meloni G, Dodge GR, Burdick JA, Schaer TP, Steinberg DR, and Mauck RL (2015) Cartilage repair and subchondral bone remodeling in response to focal lesions in a mini-pig model: implications for tissue engineering. *Tissue Eng Part A* 21, 850–860 [PubMed: 25318414]
32. Barbero A, Grogan S, Schafer D, Heberer M, Mainil-Varlet P, and Martin I (2004) Age related changes in human articular chondrocyte yield, proliferation and post-expansion chondrogenic capacity. *Osteoarthritis Cartilage* 12, 476–484 [PubMed: 15135144]
33. Huwe LW, Brown WE, Hu JC, and Athanasiou KA (2018) Characterization of costal cartilage and its suitability as a cell source for articular cartilage tissue engineering. *J Tissue Eng Regen Med* 12, 1163–1176 [PubMed: 29286211]
34. Yoon KH, Park JY, Lee JY, Lee E, Lee J, and Kim SG (2020) Costal Chondrocyte-Derived Pellet-Type Autologous Chondrocyte Implantation for Treatment of Articular Cartilage Defect. *Am J Sports Med* 48, 1236–1245 [PubMed: 32125878]
35. Kwon H, O’Leary SA, Hu JC, and Athanasiou KA (2019) Translating the application of transforming growth factor- β 1, chondroitinase-ABC, and lysyl oxidase-like 2 for mechanically robust tissue-engineered human neocartilage. *Journal of Tissue Engineering and Regenerative Medicine* 13, 283–294 [PubMed: 30557915]
36. Elder BD, and Athanasiou KA (2009) Systematic assessment of growth factor treatment on biochemical and biomechanical properties of engineered articular cartilage constructs. *Osteoarthritis Cartilage* 17, 114–123 [PubMed: 18571441]
37. Makris EA, MacBarb RF, Paschos NK, Hu JC, and Athanasiou KA (2014) Combined use of chondroitinase-ABC, TGF- β 1, and collagen crosslinking agent lysyl oxidase to engineer functional neotissues for fibrocartilage repair. *Biomaterials* 35, 6787–6796 [PubMed: 24840619]
38. Elder BD, and Athanasiou KA (2008) Synergistic and additive effects of hydrostatic pressure and growth factors on tissue formation. *PLoS one* 3, e2341 [PubMed: 18523560]
39. van der Kraan PM, Buma P, van Kuppevelt T, and van Den Berg WB (2002) Interaction of chondrocytes, extracellular matrix and growth factors: relevance for articular cartilage tissue engineering. *Osteoarthritis and Cartilage* 10, 631–637 [PubMed: 12479385]

40. Madry H, Rey-Rico A, Venkatesan JK, Johnstone B, and Cucchiari M (2014) Transforming growth factor Beta-releasing scaffolds for cartilage tissue engineering. *Tissue Eng Part B Rev* 20, 106–125 [PubMed: 23815376]
41. Blunk T, Sieminski AL, Gooch KJ, Courter DL, Hollander AP, Nahir AM, Langer R, Vunjak-Novakovic G, and Freed LE (2002) Differential effects of growth factors on tissue-engineered cartilage. *Tissue Eng* 8, 73–84 [PubMed: 11886656]
42. Moore ER, and Jacobs CR (2018) The primary cilium as a signaling nexus for growth plate function and subsequent skeletal development. *J Orthop Res* 36, 533–545 [PubMed: 28901584]
43. Elisseeff J, McIntosh W, Fu K, Blunk BT, and Langer R (2001) Controlled-release of IGF-I and TGF-beta1 in a photopolymerizing hydrogel for cartilage tissue engineering. *J Orthop Res* 19, 1098–1104 [PubMed: 11781011]
44. Mao Y, Hoffman T, Wu A, and Kohn J (2018) An Innovative Laboratory Procedure to Expand Chondrocytes with Reduced Dedifferentiation. *Cartilage* 9, 202–211 [PubMed: 29271232]
45. Lee J, Lee JY, Chae BC, Jang J, Lee E, and Son Y (2017) Fully Dedifferentiated Chondrocytes Expanded in Specific Mesenchymal Stem Cell Growth Medium with FGF2 Obtains Mesenchymal Stem Cell Phenotype In Vitro but Retains Chondrocyte Phenotype In Vivo. *Cell Transplant* 26, 1673–1687 [PubMed: 29251111]
46. Huang BJ, Brown WE, Keown T, Hu JC, and Athanasiou KA (2018) Overcoming Challenges in Engineering Large, Scaffold-Free Neocartilage with Functional Properties. *Tissue Eng Part A* 24, 1652–1662 [PubMed: 29766751]
47. Brown WE, Hu JC, and Athanasiou KA (2016) Ammonium-Chloride-Potassium Lysing Buffer Treatment of Fully Differentiated Cells Increases Cell Purity and Resulting Neotissue Functional Properties. *Tissue engineering. Part C, Methods* 22, 895–903 [PubMed: 27553086]
48. Murphy MK, Huey DJ, Reimer AJ, Hu JC, and Athanasiou KA (2013) Enhancing post-expansion chondrogenic potential of costochondral cells in self-assembled neocartilage. *PLoS One* 8, e56983 [PubMed: 23437288]
49. Murphy MK, Huey DJ, Hu JC, and Athanasiou KA (2015) TGF-beta1, GDF-5, and BMP-2 stimulation induces chondrogenesis in expanded human articular chondrocytes and marrow-derived stromal cells. *Stem Cells* 33, 762–773 [PubMed: 25377511]
50. Berson RE, Purcell MR, and Sharp MK (2008) Computationally determined shear on cells grown in orbiting culture dishes. In *Oxygen Transport to Tissue XXIX* pp. 189–198, Springer
51. Chakraborty A, Chakraborty S, Jala VR, Thomas JM, Sharp MK, Berson RE, and Haribabu B (2016) Impact of bi-axial shear on atherogenic gene expression by endothelial cells. *Annals of Biomedical Engineering* 44, 3032–3045 [PubMed: 27138524]
52. Thomas JMD, Chakraborty A, Berson RE, Shakeri M, and Sharp MK (2017) Validation of a CFD model of an orbiting culture dish with PIV and analytical solutions. *AIChE Journal* 63, 4233–4242
53. Thomas JMD, Chakraborty A, Sharp MK, and Berson RE (2011) Spatial and temporal resolution of shear in an orbiting petri dish. *Biotechnology Progress* 27, 460–465 [PubMed: 21302366]
54. Gonzalez-Leon EA, Bielajew BJ, Hu JC, and Athanasiou KA (2020) Engineering self-assembled neomenisci through combination of matrix augmentation and directional remodeling. *Acta Biomater* 109, 73–81 [PubMed: 32344175]
55. Link JM, Hu JC, and Athanasiou KA (2020) Chondroitinase ABC Enhances Integration of Self-Assembled Articular Cartilage, but Its Dosage Needs to Be Moderated Based on Neocartilage Maturity. *Cartilage*, 1947603520918653
56. Allen KD, and Athanasiou KA (2006) Viscoelastic characterization of the porcine temporomandibular joint disc under unconfined compression. *J Biomech* 39, 312–322 [PubMed: 16321633]
57. Makris EA, MacBarb RF, Responde DJ, Hu JC, and Athanasiou KA (2013) A copper sulfate and hydroxylysine treatment regimen for enhancing collagen cross-linking and biomechanical properties in engineered neocartilage. *FASEB J* 27, 2421–2430 [PubMed: 23457219]
58. Cissell DD, Link JM, Hu JC, and Athanasiou KA (2017) A Modified Hydroxyproline Assay Based on Hydrochloric Acid in Ehrlich's Solution Accurately Measures Tissue Collagen Content. *Tissue Eng Part C Methods* 23, 243–250 [PubMed: 28406755]

59. Eggenschwiler JT, and Anderson KV (2007) Cilia and Developmental Signaling. *Annual Review of Cell and Developmental Biology* 23, 345–373
60. Waller KA, Chin KE, Jay GD, Zhang LX, Teeple E, McAllister S, Badger GJ, Schmidt TA, and Fleming BC (2017) Intra-articular Recombinant Human Proteoglycan 4 Mitigates Cartilage Damage After Destabilization of the Medial Meniscus in the Yucatan Minipig. *Am J Sports Med* 45, 1512–1521 [PubMed: 28129516]
61. Christensen BB, Foldager CB, Olesen ML, Vingtoft L, Rölfing JH, Ringgaard S, and Lind M (2015) Experimental articular cartilage repair in the Göttingen minipig: the influence of multiple defects per knee. *J Exp Orthop* 2, 13 [PubMed: 26914881]
62. Otsuki S, Nakagawa K, Murakami T, Sezaki S, Sato H, Suzuki M, Okuno N, Wakama H, Kaihatsu K, and Neo M (2019) Evaluation of Meniscal Regeneration in a Mini Pig Model Treated With a Novel Polyglycolic Acid Meniscal Scaffold. *Am J Sports Med* 47, 1804–1815 [PubMed: 31172797]
63. MacBarb RF, Makris EA, Hu JC, and Athanasiou KA (2013) A chondroitinase-ABC and TGF-beta1 treatment regimen for enhancing the mechanical properties of tissue-engineered fibrocartilage. *Acta Biomater* 9, 4626–4634 [PubMed: 23041782]
64. Darling EM, and Athanasiou KA (2005) Rapid phenotypic changes in passaged articular chondrocyte subpopulations. *J Orthop Res* 23, 425–432 [PubMed: 15734258]
65. Thompson CL, Plant JC, Wann AK, Bishop CL, Novak P, Mitchison HM, Beales PL, Chapple JP, and Knight MM (2017) Chondrocyte expansion is associated with loss of primary cilia and disrupted hedgehog signalling. *Eur Cell Mater* 34, 128–141 [PubMed: 28929469]

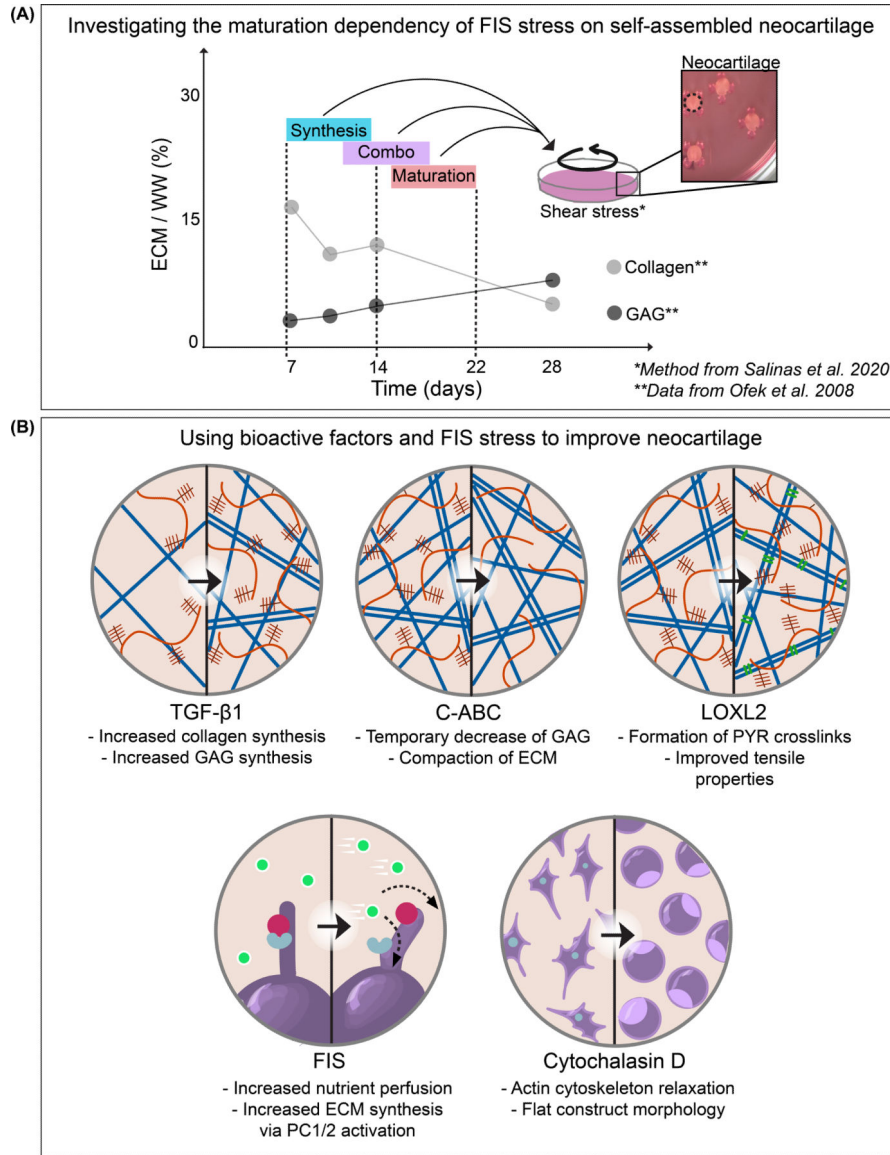


Figure 1. Maturation dependency and modes of action. a) The design of the experimental groups of Phase I follows the stages of the self-assembling process of neocartilage. The synthesis stage occurs from day 7 to day 14 of culture when glycosaminoglycan content increases slowly, and collagen content decreases slowly. During the maturation stage, from day 15 to day 22, glycosaminoglycan content continues to increase, and collagen content continues to decrease, but the total matrix production increases. The neocartilage constructs were either nonstimulated controls or stimulated with FIS stress during the synthesis stage, the maturation stage, or a combination stage (days 11–18). *Shear stress refers to fluid-induced shear stress, described previously in Salinas *et al.* (2020) (11). **Data obtained from Ofek *et al.* (2008) (23). b) Schematic representation of the modes of action for bioactive and mechanical (FIS stress) signaling factors are shown. All the bioactive and mechanical signaling factors shown were used to create the neocartilage constructs in

Phase IV. Abbreviations: chondroitinase ABC (C-ABC), combination (Combo), extracellular matrix (ECM), fluid-induced shear (FIS), glycosaminoglycan (GAG), lysyl oxidase-like 2 (LOXL2), polycystin 1/2 (PC1/2), pyridinoline (PYR), transforming growth factor beta 1 (TGF- β 1), wet weight (WW).

Author Manuscript

Author Manuscript

Author Manuscript

Author Manuscript

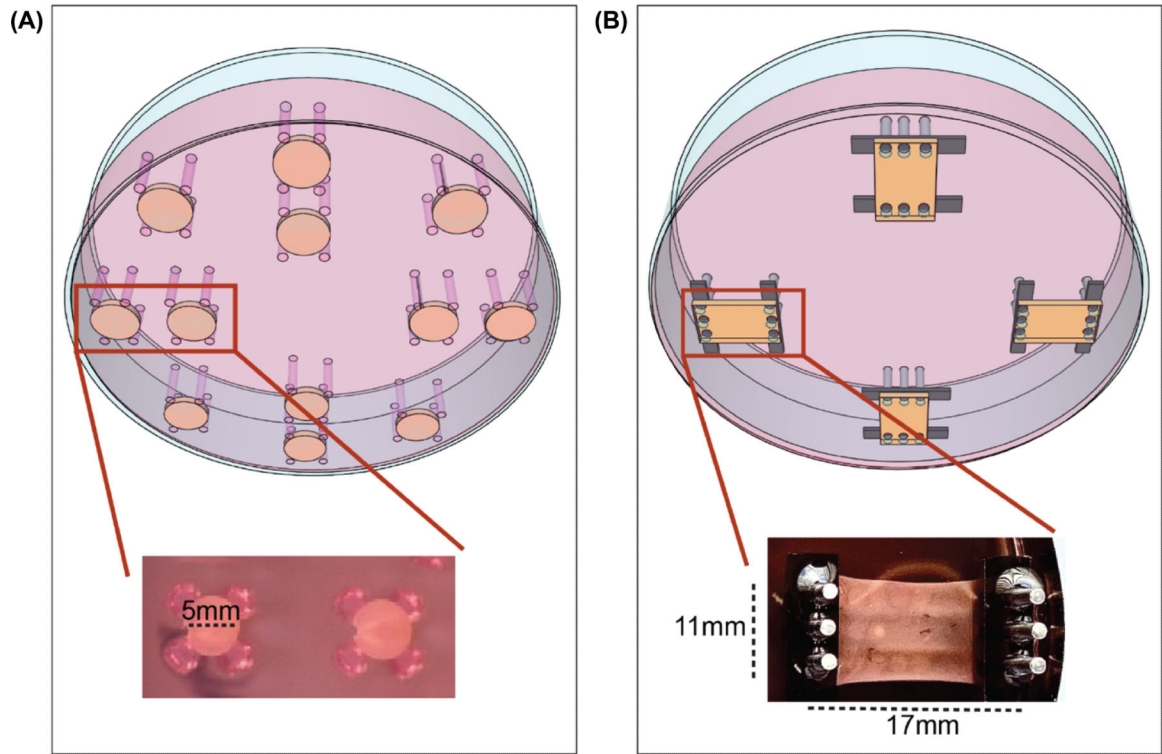
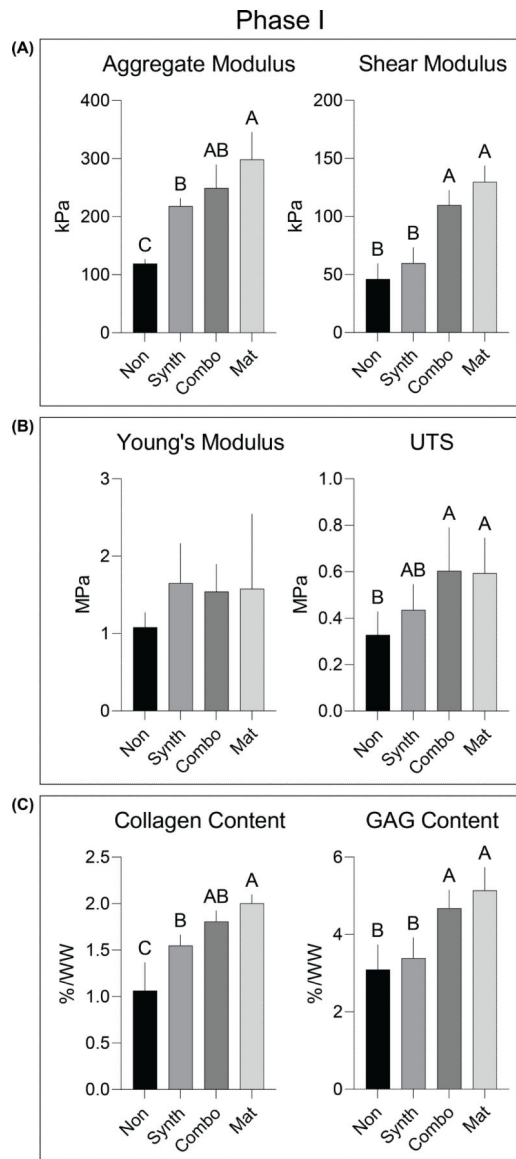


Figure 2.

The two FIS stress devices used for stimulation of circular and rectangular neocartilage constructs. a) The FIS stress device for 5mm diameter neocartilage constructs was created using a 3% agarose base inside a 100mm diameter petri dish. Neocartilage constructs of 5mm diameter were placed within four agarose posts to be held in place during FIS stress stimulation. b) A novel design of the FIS stress device was necessary to stimulate 11×17mm neocartilage constructs. The new FIS stress device was created using an acrylic base and stainless-steel metal rods. The acrylic base was placed inside a 100mm diameter petri dish, and the 11×17mm neocartilage constructs were held in place by the six metal rods and acrylic weights. Previous studies have shown that the changes created in the new design for rectangular constructs does not significantly alter the fluid flow or FIS stress applied to the neocartilage (50–53). For both designs, previous computational fluid dynamic modeling studies have shown that a speed of 50RPM on an orbital shaker achieves 0.05–0.21Pa of FIS stress on neocartilage constructs (11).

**Figure 3.**

Identifying the best time of application for FIS stress. Phase I constructs were derived from bovine articular chondrocytes in small 5mm diameter circular shapes and included four groups to determine an optimal FIS stress stimulation stage: nonstimulated, stimulated with FIS stress during the synthesis stage, stimulated with FIS stress during the maturation stage, and stimulated with FIS stress during combination of synthesis and maturation stages. a) The aggregate modulus and shear modulus under compressive conditions, b) the Young's modulus and the ultimate tensile strength under tensile conditions, c) and the collagen content and the glycosaminoglycan content of neocartilage constructs are shown. Bars not sharing the same letter are statistically different when evaluated at $p < 0.05$ using a one-way ANOVA and Tukey's *post hoc* test. Abbreviations: combination (Combo), glycosaminoglycan (GAG), kilopascals (kPa), maturation stage (Mat), megapascals (MPa), nonstimulated (Non), synthesis stage (Synth), percent by wet weight (%/WW).

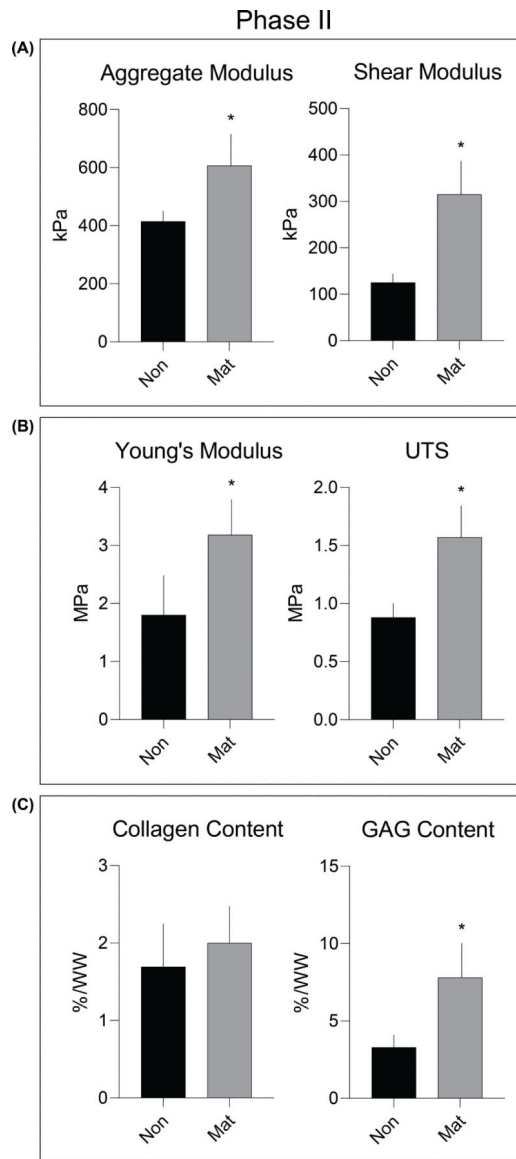


Figure 4.

Translating FIS stress stimulation to costal chondrocytes from the Yucatan minipig. Phase II constructs were derived from passage 3 minipig costal chondrocytes in small 5mm diameter circular shapes and included two groups to assess the translatability of the FIS stress stimulation regimen across cell sources and species: nonstimulated and stimulated with FIS stress during the maturation stage. a) The aggregate modulus and the shear modulus under compressive conditions, b) the Young's modulus and the ultimate tensile strength under tensile conditions, c) and the collagen content and the glycosaminoglycan content of neocartilage constructs are shown. The asterisk (*) above the bars indicates statistically different groups when evaluated at $p < 0.05$ using Student's t -test. Abbreviations: glycosaminoglycan (GAG), kilopascals (kPa), maturation stage (Mat), megapascals (MPa), nonstimulated (Non), percent per wet weight (%/WW).

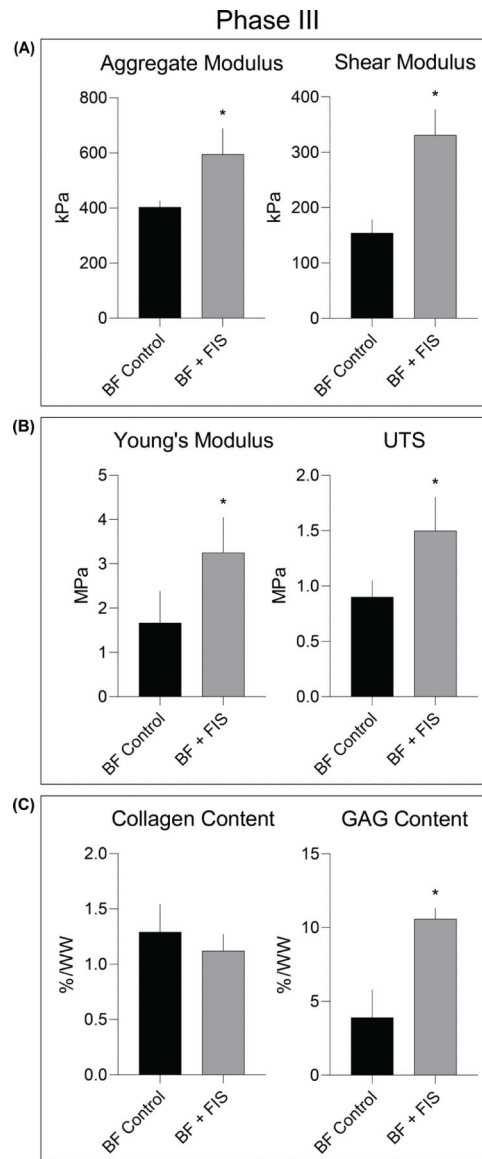


Figure 5.

Combining bioactive factors and FIS stress to further improve the functional properties of neocartilage constructs. Phase III constructs were derived from passage 3 minipig costal chondrocytes in small 5mm diameter circular shapes and included two groups: treated with bioactive factors alone, and treated with bioactive factors and FIS stress stimulation during the maturation stage. a) The aggregate modulus and the shear modulus under compressive conditions, b) the Young's modulus and the ultimate tensile strength under tensile conditions, c) and the collagen content and the glycosaminoglycan content of neocartilage constructs are shown. The asterisk (*) above the bars indicate statistically different groups when evaluated at $p < 0.05$ using Student's t -test. Abbreviations: bioactive factors (BF), fluid-induced shear (FIS), glycosaminoglycan (GAG), kilopascals (kPa), megapascals (MPa), percent per wet weight (%/WW).

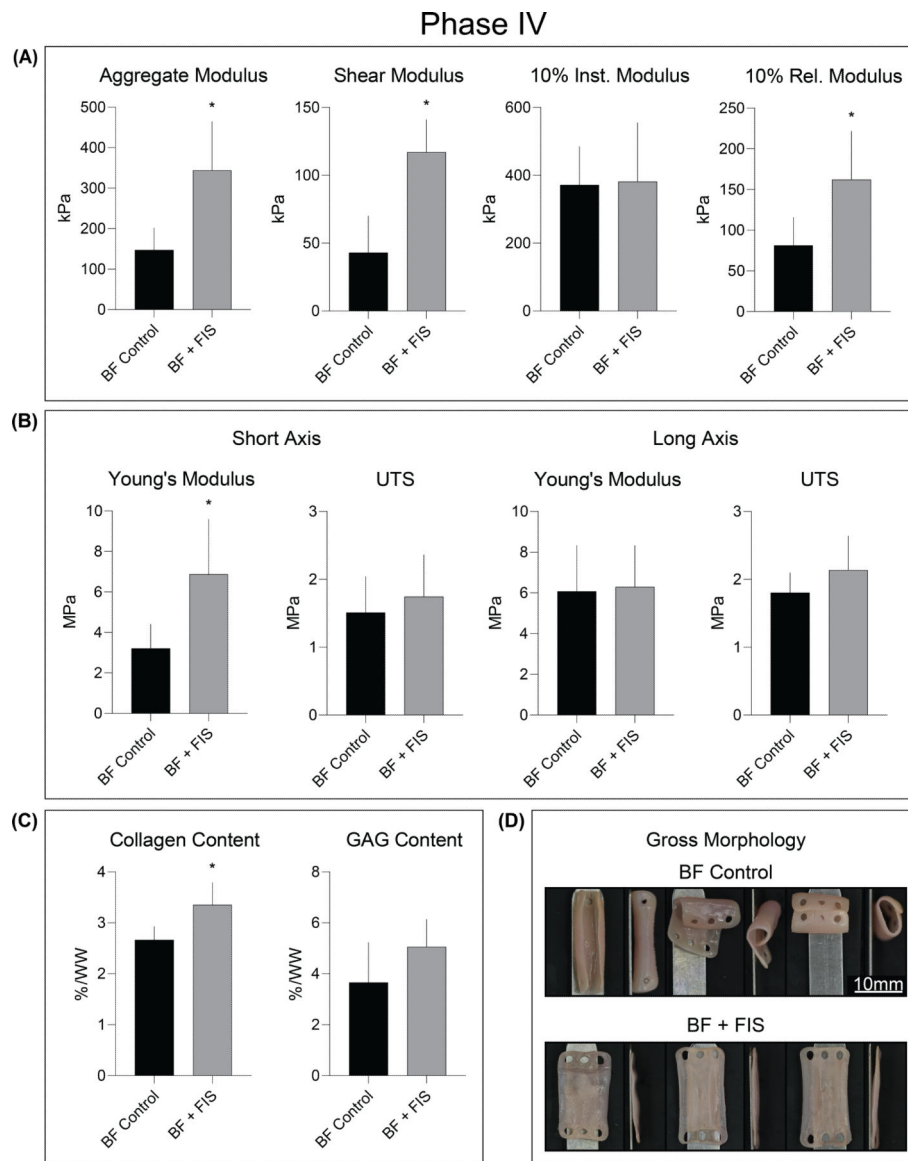


Figure 6. Scaling-up the size of neocartilage constructs created from highly passaged chondrocytes using FIS stress and bioactive factors. Phase IV constructs were derived from passage 6 minipig costal chondrocytes in 11×17mm rectangular shapes and included two groups: treated with bioactive factors plus cytochalasin D, and treated with bioactive factors, cytochalasin D, plus FIS stress stimulation during the maturation stage. a) The aggregate modulus, the shear modulus, and the 10% instantaneous and relaxation moduli under compressive conditions, b) and the Young's modulus and the ultimate tensile strength for both the long and short axis of neocartilage constructs under tensile conditions are shown. c) The collagen content and the glycosaminoglycan content, and d) images of the gross morphology of neocartilage constructs are shown. The asterisk (*) above the bars indicates statistically different groups when evaluated at $p < 0.05$ using Student's t -test. Abbreviations: bioactive factors (BF), fluid-induced shear (FIS), instantaneous (Inst.),

glycosaminoglycan (GAG), kilopascals (kPa), megapascals (MPa), percent per wet weight (%/WW), relaxation (Rel.).

Author Manuscript

Author Manuscript

Author Manuscript

Author Manuscript

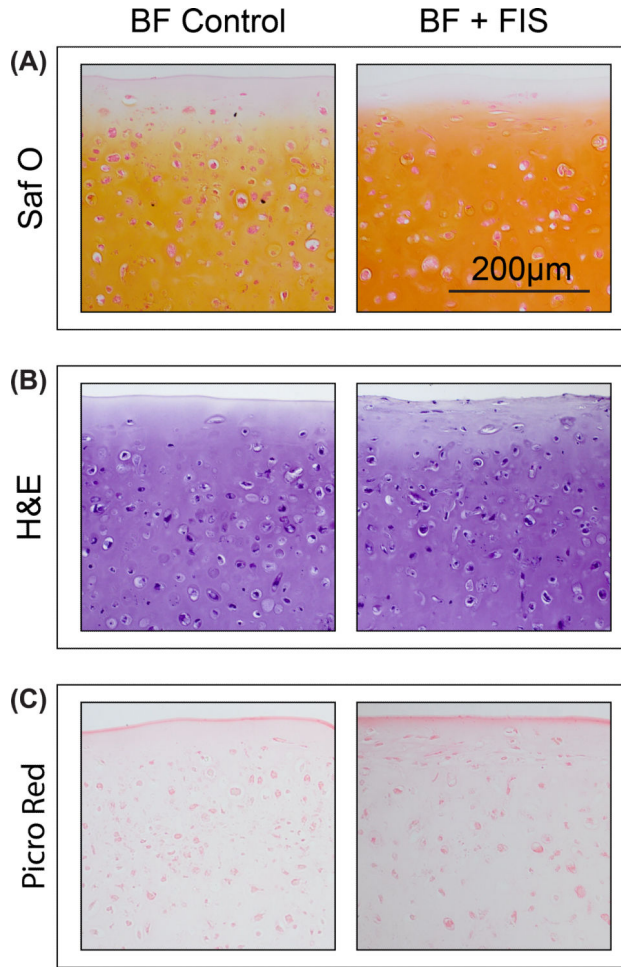


Figure 7. Combining bioactive factors and FIS stress increases intensity for glycosaminoglycan staining. Phase IV constructs were derived from passage 6 minipig costal chondrocytes in 11×17mm rectangular shapes and included two groups: treated with bioactive factors plus cytochalasin D, and treated with bioactive factors, cytochalasin D, plus FIS stress stimulation during the maturation stage. Representative images of a) safranin O staining for glycosaminoglycan content, b) hematoxylin and eosin staining for general cellular and tissue morphology, and c) picrosirius red staining for general collagen content are shown. Abbreviations: bioactive factors (BF), fluid-induced shear (FIS), hematoxylin and eosin (H&E), picrosirius red (Picro Red), safranin O (Saf O).

Table 1.

Timeline of FIS stress and bioactive factor application. The specific timeline of application for FIS stress, TGF- β 1, C-ABC, LOXL2, and cytochalasin D is shown. Abbreviations: chondroitinase ABC (C-ABC), lysyl oxidase-like 2 (LOXL2), transforming growth factor beta 1 (TGF- β 1).

Treatment	Time					
	Week 1	Week 2	Week 3	Week 4	Week 5	Week 6
Phase I:						
Synthesis		■				
Combination		■	■			
Maturation			■	■		
Phase II:						
Maturation			■	■		
Phase III:						
Maturation			■	■		
TGF- β 1	■	■	■	■		
C-ABC		■				
LOXL2		■	■			
Phase IV:						
Maturation			■	■		
TGF- β 1	■	■	■	■		
C-ABC		■				
LOXL2		■	■			
Cytochalasin D	■					

Author Manuscript

Author Manuscript

Author Manuscript

Author Manuscript